Na^+ Permeation and Block of hERG Potassium Channels

Hongying Gang and Shetuan Zhang

Institute of Cardiovascular Sciences, St. Boniface General Hospital Research Centre, and Department of Physiology, Faculty of Medicine, University of Manitoba, Winnipeg, Manitoba, Canada R2H 2A6

The inactivation gating of hERG channels is important for the channel function and drug–channel interaction. Whereas hERG channels are highly selective for K^+, we have found that inactivated hERG channels allow Na^+ to permeate in the absence of K^+. This provides a new way to directly monitor and investigate hERG inactivation. By using whole cell patch clamp method with an internal solution containing 135 mM Na^+ and an external solution containing 135 mM NMG^+, we recorded a robust Na^+ current through hERG channels expressed in HEK 293 cells. Kinetic analyses of the hERG Na^+ and K^+ currents indicate that the channel experiences at least two states during the inactivation process, an initial fast, less stable state followed by a slow, more stable state. The Na^+ current reflects Na^+ ions permeating through the fast inactivated state but not through the slow inactivated state or open state. Thus the hERG Na^+ current displayed a slow inactivation as the channels travel from the less stable, fast inactivated state into the more stable, slow inactivated state. Removal of fast inactivation by the S631A mutation abolished the Na^+ current. Moreover, acceleration of fast inactivation by mutations T623A, F627Y, and S641A did not affect the hERG Na^+ current, but greatly diminished the hERG K^+ current. We also found that external Na^+ potently blocked the hERG outward Na^+ current with an IC_{50} of 3.5 mM. Mutations in the channel pore and S6 regions, such as S624A, F627Y, and S641A, abolished the inhibitory effects of external Na^+ on the hERG Na^+ current. Na^+ permeation and blockade of hERG channels provide novel ways to extend our understanding of the hERG gating mechanisms.

The Journal of General Physiology

INTRODUCTION

hERG (human ether-a-go-go-related gene) encodes a voltage-gated K^+ channel existing in a number of cell types including neurons, cardiac myocytes, and tumor cells (Sanguinetti et al., 1995; Trudeau et al., 1995; Faravelli et al., 1996; Bianchi et al., 1998). In the heart, hERG channels conduct the rapidly activating delayed rectifier K^+ current (I_{Kr}), which is important for cardiac repolarization (Sanguinetti and Jurkiewicz, 1990; Sanguinetti et al., 1995). Reduction of I_{Kr} induced by mutations in hERG or drug block slows repolarization, causing long QT syndrome and sudden cardiac death (Keating and Sanguinetti, 2001). The inactivation gating of hERG is particularly important for channel function and drug–channel interaction. The fast voltage-dependent inactivation limits outward current through the channel at positive voltages and thus helps maintain the action potential plateau phase that controls contraction and prevents premature excitation. As well, hERG inactivation gating is involved in high affinity binding of many drugs to the channel.

The inactivation of hERG channels resembles the C-type inactivation of *Shaker* K^+ channels in its sensitivity to extracellular K^+ concentration and TEA, and to mutations in the P-loop (Hoshi et al., 1991; Smith et al., 1996; Schönherr and Heinemann, 1996; Fan et al., 1999). The C-type inactivation of K^+ channels is not well understood, and seems to involve either multiple mechanisms or a single mechanism with multiple steps (Olcese et al., 1997; Yang et al., 1997b; Loots and Isacoff, 1998; Kiss et al., 1999; Wang and Fedida, 2001). For example, Loots and Isacoff (1998) have shown that C-type inactivation contains a faster closing of the channel pore and a much slower gating charge immobilization. To describe the complexity of the C-type inactivation process, the term P-type inactivation has been used to refer to the initial closure of the channel pore, and the C-type inactivation has also been assigned to specifically mean the stabilized inactivated conformation of the channel (De Biasi et al., 1993; Loots and Isacoff, 1998). In this concept, P-type inactivation appears to occur in a limited region of the channel pore and eliminate K^+ currents without inducing substantial conformational changes in the channel. Recently, Berneche and Roux (2005) showed that the selectivity filter of the K^+ channel can undergo a transition involving two amide planes of one subunit (Val76-Gly77 and Thr75-Val76 in KcsA), which breaks the fourfold symmetry of the tetrameric channel and contributes to the channel inactivation. It has been shown that gating charge of P-type inactivated channels is not immobilized (Yang et al., 1997b). C-type inactivation may reflect a stabilized P-type inactivation,

Correspondence to Shetuan Zhang: szhang@sbrc.ca

Abbreviations used in this paper: HEK, human embryonic kidney; hERG, human ether-a-go-go–related gene; WT, wild type.

involving a further conformational change of the channel pore that stabilizes the S4 segments in the activated or outward position (Olcese et al., 1997; Wang and Fedida, 2001). Consistent with this notion, Yang et al. (1997b) presented evidence that P- and C-type inactivations are different from each other. They showed that the nonconducting W434F *Shaker* mutant is in a permanently inactivated state (P-type) but not in a permanently charge-immobilized (C-type) state. However, most data of ionic current analyses from Kv channels are not sufficient to differentiate P- from C-type inactivation because both of them are non-K^+ conducting states.

Studies on *Shaker*, Kv2.1, and Kv1.5 K^+ channels have revealed that these channels become Na^+ permeable during inactivation in the absence of K^+ (Korn and Ikeda, 1995; Starkus, J.G., M.D. Rayner, and S.H. Heinemann. 1997. *Biophys. J.* 72:A232; Starkus et al., 1998; Kiss et al., 1999; Wang et al., 2000). It has been proposed that during C-type inactivation, the channels undergo three conformational states: an initial open state that is highly selective for K^+, an intermediate inactivation state that is less permeable to K^+ but more permeable to Na^+, and a final more stable inactivation state that is nonconducting (Starkus, J.G., M.D. Rayner, and S.H. Heinemann. 1997. *Biophys. J.* 72:A232; Loots and Isacoff, 1998; Kiss et al., 1999; Wang et al., 2000; Wang and Fedida, 2001). Since hERG inactivation resembles the C-type inactivation of *Shaker* channels (Hoshi et al., 1991; Schönherr and Heinemann, 1996; Smith et al., 1996; Spector et al., 1996), we proposed that the hERG channel allows Na^+ to permeate during the inactivation process. With an intracellular solution containing 135 mM Na^+ and an extracellular solution containing 135 mM membrane-impermeable NMG^+, we have recorded a robust Na^+ current. Gating kinetic and mutational analyses suggested that hERG channels undergo at least two inactivation steps. The less stable, P-type inactivated state is quickly reached upon depolarization, and is followed by a slow entry into the more stable C-type inactivated state. The P-type inactivated state is the Na^+ permeating state, while the C-type inactivated state is nonconducting. We further found that the hERG Na^+ current can be blocked by external Na^+, and the residues in the channel pore and S6 regions, including the serine residues at 624 and 641 as well as the phenylalanine in the signature motif of the selectivity filter, are involved in the block.

MATERIALS AND METHODS

Molecular Biology

hERG cDNA in pcDNA3 was obtained from G.A. Robertson (University of Wisconsin-Madison, Madison, WI; Trudeau et al., 1995). Mutations in the pore loop and S6 were constructed to assess the role of inactivation as well as the sites involved in the Na^+ permeation and block of the channel. The T623A, F627Y, and S641A were constructed to accelerate hERG inactivation. The T623A and S641A have been shown to speed up hERG inactivation (Mitcheson et al., 2000; Bian et al., 2004), and we recently discovered that the F627Y also significantly accelerates hERG inactivation (Guo et al., 2006). The S631A mutation was used to remove hERG inactivation gating (Schönherr and Heinemann, 1996; Smith et al., 1996; Herzberg et al., 1998). The S624A mutation was used to assess the interaction between external Na^+ and hERG channels (Mullins et al., 2002). Point mutations of hERG were generated by PCR using the overlap extension technique (Ho et al., 1989). The forward and reverse flanking primers were designed to cover two unique restriction sites (BstEII at nucleotide 2038 and SbfI at nucleotide 3093). The first round of PCRs was performed using the forward flanking primer-reverse mutant primer, and the reverse flanking primer-forward mutant primer, respectively. The resulting two PCR products were then used as templates and amplified by flanking primers in a second round of PCR. The final PCR product was cloned into Zero Blunt Vector (Invitrogen). A 1,055-bp fragment containing the point mutation was cut by BstEII and SbfI (New England Biolabs, Inc.), and then subcloned into the pcDNA3 vector containing the wild-type (WT) hERG at the same sites (Lin et al., 2005). All mutations were verified using a high-throughput 48 capillary ABI 3730 sequencer (UCDNA Services, University of Calgary).

hERG mutant channels were transiently expressed in HEK 293 cells (American Type Culture Collection). HEK 293 cells were seeded at 5×10^5 cells/60-mm diameter dish. The cells were transiently transfected using 10 μl lipofectamine with 4 μg hERG mutant cDNA in pcDNA3 vector. After 24–48 h, 30–80% of cells expressed channels. Nontransfected HEK 293 cells contain a small-amplitude background K^+ current that is usually <100 pA upon a depolarizing pulse to 50 mV. Thus, the effects of overlapping endogenous currents of HEK 293 cells on the expressed current are minimal. A HEK 293 cell line stably expressing hERG channels obtained from C. January (University of Wisconsin-Madison) (Zhou et al., 1998) was also used. In this cell line, the hERG cDNA (Trudeau et al., 1995) was subcloned into BamHI/EcoRI sites of the pcDNA3 vector (Invitrogen). The stably transfected cells were cultured in minimum essential medium (MEM) supplemented with 10% FBS and contained 400 μg/ml G418 (Sigma-Aldrich) to select for transfected cells. For electrophysiological study, the cells were harvested from the culture dish by trypsinization and stored in standard MEM medium at room temperature. Cells were studied within 8 h of harvest.

Patch Clamp Recording Method

The whole cell patch clamp method was used. The pipette solution contained (in mM) 135 NaCl, 5 EGTA, 1 $MgCl_2$, 10 HEPES, and was adjusted to pH 7.2 with NaOH. The bath solution contained (in mM) 10 HEPES, 10 glucose, 1 $MgCl_2$, 2 $CaCl_2$, 135 NMG^+, and was adjusted to pH 7.4 with HCl. For recordings in the presence of different external K^+ or Na^+ concentrations, the concentration of NMG^+ was proportionally reduced as the K^+ or Na^+ concentration was elevated to maintain a constant osmolarity, and the pH was adjusted to 7.4 with the appropriate hydroxide solution. All chemicals were purchased from Sigma-Aldrich. Throughout the text the subscripts i and o denote intra- and extracellular ion concentrations, respectively.

Aliquots of cells were allowed to settle on the bottom of a <0.5-ml cell bath mounted on an inverted microscope (TE2000; Nikon). Cells were superfused with specific bath solutions. The bath solution was constantly flowing through the chamber and the solution was changed by switching the perfusates at the inlet of the chamber, with complete bath solution change taking 10 s. Patch electrodes were fabricated using thin-walled borosilicate glass (World Precision Instruments). The pipettes had inner diameters of ~1.5 μm and resistances of ~2 MΩ when filled with pipette solutions. An Axopatch 200B amplifier was used to record

membrane currents. Computer software (pCLAMP9; Axon Instruments) was used to generate voltage clamp protocols, acquire data, and analyze current signals. Data were filtered at 5–10 kHz and sampled at 20–50 kHz for all protocols. Typically, 80% series resistance (R_s) compensation was used and leak subtraction was not used. Conductance/voltage data were fitted to a single Boltzmann function, $y = 1/(1 + \exp((V_{1/2} - V)/k))$, where y is the current normalized with respect to the maximal tail current, $V_{1/2}$ is the half-activation potential or midpoint of the activation curve, V is the voltage during the prepulse, and k is the slope factor in mV, reflecting the steepness of the voltage dependence of gating. Curve fitting was done using multiple nonlinear least squares regression analysis. Concentration effects of external Na^+ (Na^+_o) on the WT Na^+ current were quantified by fitting data to the Hill equation, $I_{Na}/I_{control} = 1/[1 + (D/IC_{50})^H]$, where D is the Na^+_o concentration, IC_{50} is the Na^+_o concentration for 50% block, and H is the Hill coefficient to the results. Data are given as mean ± SEM. Clampfit (Axon Instruments) and Origin (OriginLab) were used for data analysis. All experiments were performed at room temperature (23 ± 1°C).

RESULTS

Na^+ Permeation through hERG K^+ Channels

Under ionic conditions with a pipette solution containing 135 mM Na^+ and a bath solution containing 135 mM NMG^+ without K^+ or Na^+, we have consistently recorded robust Na^+ currents in hERG-expressing HEK 293 cells. In Fig. 1 A, Na^+ currents were activated by 4-s depolarizing pulses from a holding potential of −80 mV to voltages between −70 and 70 mV in 10-mV increments. The depolarizing pulses were followed by a repolarizing step to −50 mV. In contrast to the hERG K^+ current, the hERG Na^+ current increased in amplitude as the depolarizing voltage increased (Fig. 1 A). The Na^+ current was sensitive to the specific hERG blockers. As shown in Fig. 1 B, the current was completely blocked by 1 μM astemizole ($n = 5$). The current was also sensitive to the methanesulfonanilide drug E-4031 (unpublished data). In the nontransfected HEK 293 cells, no Na^+ current could be detected (Fig. 1 C, $n = 6$). Contamination of Cl^- current was ruled out because the Na^+ current in hERG-HEK cells was not affected by the bath application of 100 μM DIDS, a Cl^- channel blocker. As well, changing Cl^- concentration by glutamic substitution had no effect on the current. The Na^+ current was essentially the same when a pipette solution containing 135 mM Na-glutamate instead of 135 NaCl was used ($n = 4$; unpublished data). These results indicate that the Na^+ current reflects Na^+ permeation through hERG channels. Fig. 1 D shows the current–voltage (I-V) relationships of the hERG Na^+ current amplitudes at peak (▲) and at the end of depolarizing steps (●) in 13 cells. Notably, the I-V relationships of the hERG Na^+ current are nearly ohmic, which are different from the inward rectification of the I-V relationships of the hERG K^+ current.

To further address whether the Na^+ permeating hERG channels are K^+ selective, we studied the effects

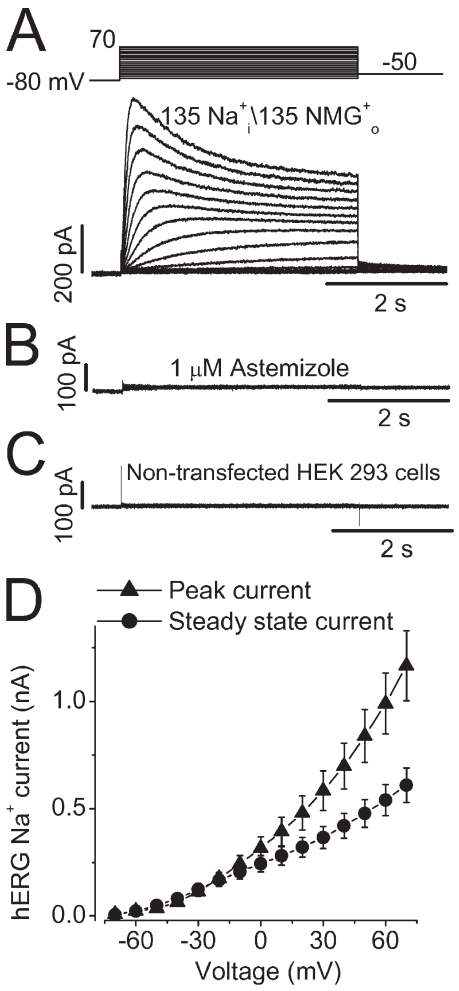

Figure 1. Na^+ permeation through hERG potassium channels. (A) Na^+ currents were elicited by depolarizing voltage steps from hERG channels stably expressed in HEK 293 cells. The pipette solution contained 135 mM Na^+ and the bath solution contained 135 mM NMG^+ as major cations. (B) Na^+ currents recorded from the hERG-HEK 293 cells were completely blocked by 1 μM astemizole, a specific hERG blocker. (C) No Na^+ current could be detected in the nontransfected HEK 293 cells. (D) Current–voltage (I-V) relationships for the peak (▲) and steady-state (●) hERG Na^+ currents recorded during the 4-s depolarization pulses ($n = 13$, data points and error bars signify mean ± SEM).

of external K^+ (K^+_o) on the Na^+ current. K^+_o inhibits the outward Na^+ current with a K_D of 0.61 ± 0.08 mM and a slope factor of 1.42 ± 0.17 ($n = 7$, Fig. 2). Upon repolarization, the inward K^+ tail current appears and this inward current was completely abolished by 100 nM E-4031. These results indicate that hERG channels were intact and not "defunct" when Na^+ permeates (Almers and Armstrong, 1980; Melishchuk et al., 1998).

To characterize hERG Na^+ current, we examined the time courses of current activation, deactivation, onset of inactivation, and recovery from inactivation. The time courses of the current activation are apparently sigmoidal (Fig. 3 A). The initial sigmoidal component is

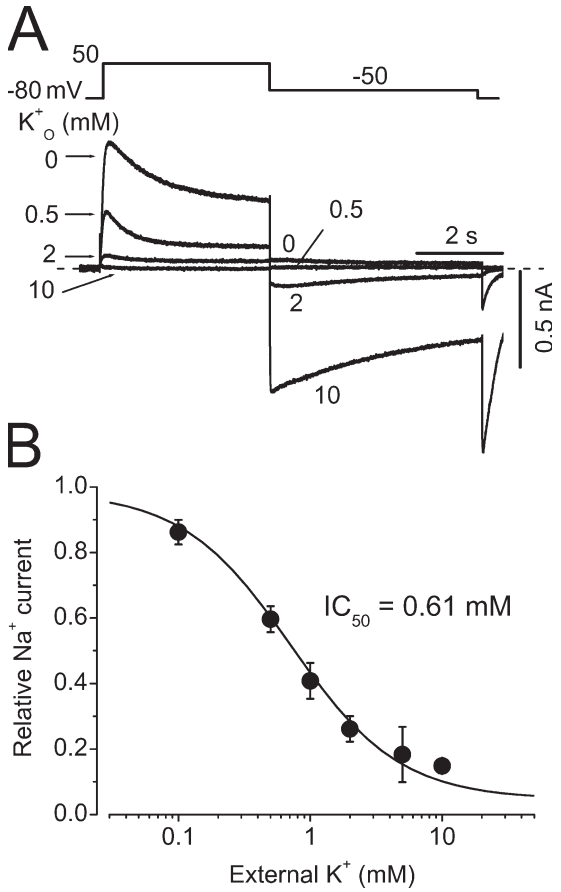

Figure 2. Inhibition of hERG Na^+ currents by extracellular K^+ (K^+_o). (A) Superimposed current traces with constant 135 mM Na^+_i and varying K^+_o. (B) Concentration-dependent inhibition of outward Na^+ currents by K^+_o ($n = 7$).

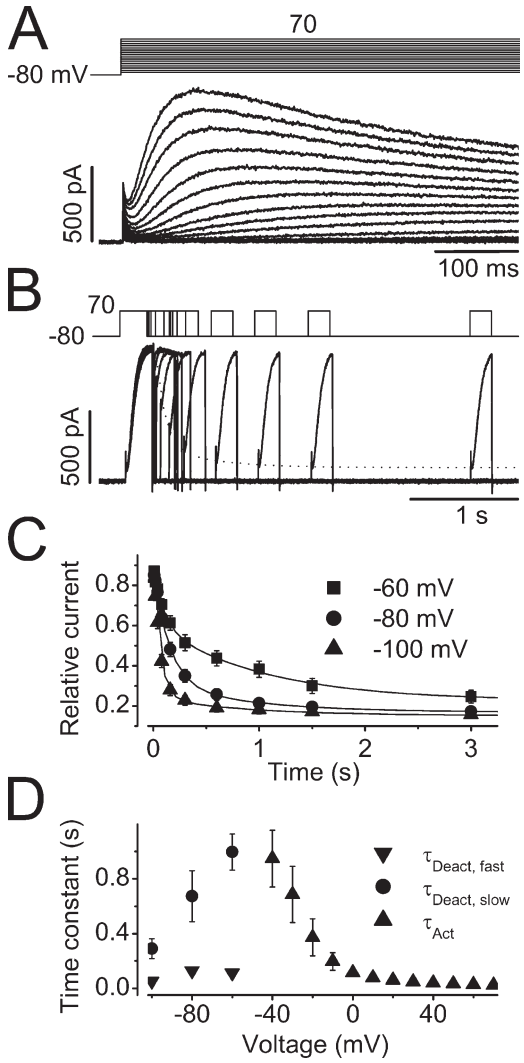

Figure 3. Time courses of hERG Na^+ current activation and deactivation. (A) The initial phase of the Na^+ currents during the depolarizing pulses ranging from −70 to 70 mV in 10-mV increments. The activation time constants were estimated by fitting the rising phase of each current trace to a single exponential function with the initial sigmoidal component ignored ($n = 13$). (B) A three-pulse protocol was used to study the hERG Na^+ current deactivation. After a peak current was reached by the initial depolarizing pulse to 70 mV (P1), the cell was clamped to −80 mV (P2) for different periods of time before it was depolarized to 70 mV (P3) to monitor the channel deactivation. The dotted line indicates the double exponential fit to the instantaneous current amplitudes upon P3. (C) The amplitude of the initial current during P3 was plotted against the time periods of P2 at −60, −80, and −100 mV, fitted to double exponential functions to obtain time constants of deactivation at −60 (■), −80 (●), and −100 mV (▲) ($n = 7$). (D) Voltage dependence of the time constants of activation (▲), and fast (▼) and slow (●) components of deactivation.

ignored and the single exponential is fitted to the remainder major portion of the current to obtain the activation time constant (τ_{act}) at various voltages. The voltage dependence of the τ_{act} of the Na^+ current is summarized in Fig. 3 D (▲, $n = 13$).

Due to the extremely small tail current at negative voltages, deactivation properties of the hERG Na^+ current were studied using a three-pulse protocol as shown in Fig. 3 B. From the holding potential of −80 mV, a depolarization to 70 mV for 250 ms (P1 pulse) was used to maximally activate the channels (to induce the peak amplitude). The cells were then repolarized to test potentials for various durations (P2 pulse) for channels to deactivate. The cell membrane was then depolarized to 70 mV again for 200 ms (P3 pulse) to monitor the instantaneous current amplitudes that represent the proportion of not yet deactivated channels during P2. The instantaneous current amplitudes upon P3 are plotted against the duration of P2 at −60, −80, and −100 mV (Fig. 3 C). As the P2 prolongs, instantaneous current upon the P3 decreases, reflecting the channel deactivation during P2. The data points were fitted to the double exponential function, and the deactivation time constants (τ_{deact}) were obtained. The voltage dependence of τ_{deact} of the hERG Na^+ current is shown in Fig. 3 D (▼, ●; $n = 7$).

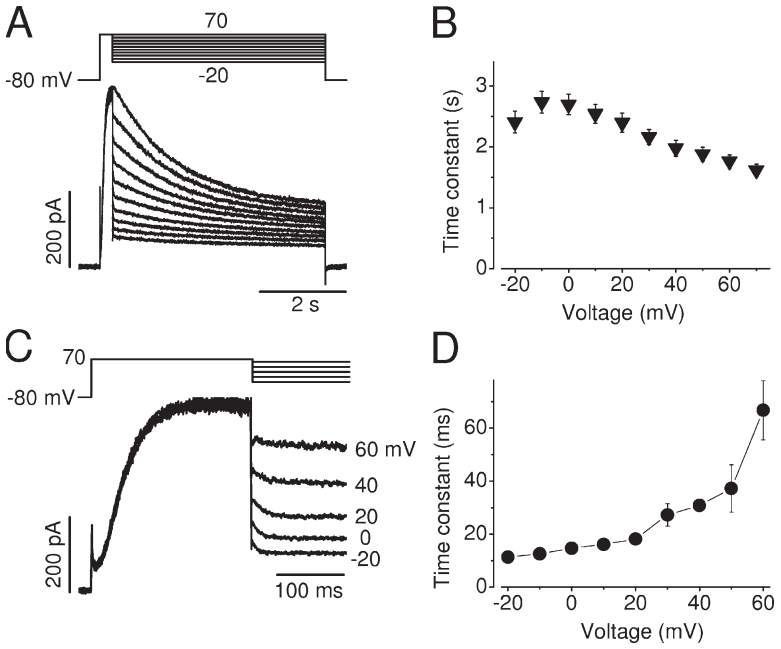

Figure 4. Voltage-dependent fast and slow decay of the hERG Na^+ current. (A) Cells were held at −80 mV and depolarized to 70 mV for 250 ms to induce the maximal hERG Na^+ currents. Test pulses were followed at potentials ranging from −20 to 70 mV in 10-mV increments. Current decays during 5-s test pulses were fitted to a single exponential function to obtain the time constants. (B) Voltage dependence of the averaged slow decay time constants from nine cells. (C) hERG Na^+ current during the voltage changes from 70 mV to various test potentials. hERG Na^+ current was evoked by a depolarizing step to 70 mV for 250 ms, immediately followed by test potentials between −20 and 60 mV. The rapid decay of the Na^+ current upon various test potentials was fitted to a single exponential function to obtain time constants. (D) The voltage dependence of the time constants of the rapid Na^+ current decay ($n = 6$ cells for each voltage). hERG currents were recorded with a pipette solution containing 135 mM Na^+ and a bath solution containing 135 mM NMG^+.

During sustained depolarizations, the hERG Na^+ current displayed a decay phase that may represent a slow inactivation (Fig. 1 A). To examine the voltage dependence of the hERG Na^+ current inactivation, a depolarizing step to 70 mV for 250 ms was used to induce the peak Na^+ current. The cells were then clamped to various voltages for 4 s to record the time course of the current decay, which was fitted to a single exponential function (Fig. 4 A). The time constants of the hERG Na^+ current inactivation (τ_{inact}) were plotted against the test voltages (Fig. 4 B). Two features of Na^+ current inactivation are prominent; first, in contrast to the inactivation of hERG K^+ currents, the inactivation of hERG Na^+ currents is only weakly voltage dependent. Second, the τ_{inact} is nearly 1,000-fold slower than that of the hERG K^+ current ($n = 9$).

Inactivation of the hERG K^+ current is very fast (time constant in millisecond ranges) and strongly voltage dependent, leading to the characteristic inward rectification of the current–voltage relationships (Sanguinetti et al., 1995; Trudeau et al., 1995). However, stronger depolarizing steps evoke larger outward hERG Na^+ currents with a slow decay (Fig. 1, A and D). One of the explanations for this result is that the hERG Na^+ current represents Na^+ permeating through the inactivated hERG channels. Because we have also found that the Na^+ current slowly inactivates during the prolonged depolarizations (Fig. 4, A and B), which mimics the typical C-type inactivation in *Shaker*, we propose that inactivation of the hERG channel involves at least two steps, the fast entry into the less stable, P-type inactivated state, and the slow entry into the more stable C-type inactivated state. We propose that Na^+ permeates through the fast inactivated state (P-type) but not through either open state or C-type inactivated state. Since P-type inactivation of the hERG channel occurs faster than channel opening, activation of the Na^+ current reflects transition from the closed state to the P-type inactivated state through the open state. We believe that the Na^+ current decay during depolarizations reflects the entry of the P-type inactivated channels into the C-type inactivated state.

The notion that Na^+ permeates through the P-type inactivated state but not the open state is supported by the data shown in Fig. 4. Careful inspection of the current traces in Fig. 4 A indicated a fast decay of the Na^+ current immediately upon voltage changes from the initial depolarization of 70 mV. The portion of the Na^+ current traces during the 70-mV depolarization and immediately upon voltage changes are expanded in Fig. 4 C. The fast decay of the Na^+ currents upon test pulses (Fig. 4 C) was fitted to a single exponential function, and the time constants were plotted against the test voltages (Fig. 4 D, $n = 6$). We believe that the fast decay of Na^+ currents represents the recovery of P-type inactivated channels (Na^+ permeable) to the "open" state, which is Na^+ impermeable. Consistently, the time constants of the fast Na^+ current decay were much smaller than those of the Na^+ current deactivation (Fig. 3) but comparable with those of recovery from inactivation of hERG channels (Zhang et al., 2003a, also see Fig. 7). Since hERG inactivation is voltage dependent, changing the voltage step from 70 mV to less depolarizing voltages would cause recovery of the P-type inactivated channels to the open state. In brief, at steady state during the last pulse in Fig. 4 C, the current represents the fraction of channels in the P-type inactivated state. At the beginning of that pulse, there is a relaxation

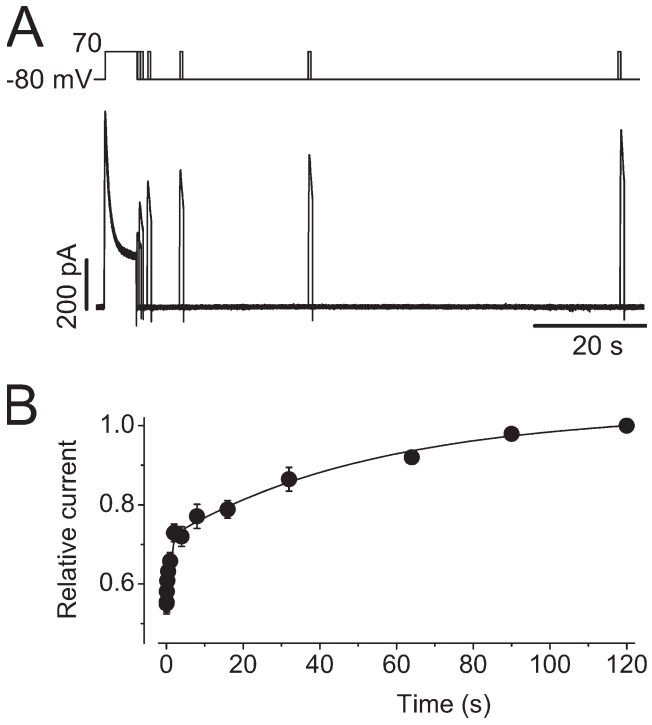

Figure 5. Time course of recovery from inactivation of the hERG Na^+ current. (A) Voltage protocol and the Na^+ currents for studying recovery from inactivation. From a holding potential of −80 mV, the cell was depolarized to 70 mV for 6 s until steady-state inactivation was reached. The cell was then clamped to −80 mV for different periods of time before it was depolarized to 70 mV for 800 ms to observe channel recovery. The interpulse interval was 120 s. (B) Time-dependent recovery of the Na^+ current. The superimposed line represents the best fit of the averaged data from 13 cells to double exponential functions.

to a lower current level, the reduction of which represents the fraction channels exiting the inactivated state and moving into the open state. This decrease in current indicates that the Na^+ current does not permeate through the open state.

We have shown that Na^+ current displayed a slow inactivation with time constants ranging from 2.7 to 1.6 s at voltages between −20 and 70 mV (Fig. 4, A and B). To evaluate the recovery from inactivation, a 6-s depolarizing pulse to 70 mV (P1) was used to induce a steady-state inactivation. The cells were then repolarized to −80 mV for various periods of time (P2), and then the cells were depolarized to 70 mV for 800 ms (P3) to measure the channel recovery (Fig. 5 A). The peak amplitude of the Na^+ current upon P3 was plotted against the duration of P2, and the data points were fitted to the double exponential function to obtain the time constants of recovery from inactivation (τ_{rec}, Fig. 5 B). The τ_{rec} at −80 mV were 0.7 ± 0.1 s and 54 ± 12 s (n = 13). Thus, recovery from inactivation of the Na^+ currents is also nearly 1,000-fold slower than that of the K^+ current (Zhang et al., 2003a; Lin et al., 2005). These results again indicate that the slow Na^+ current decay may reflect the channel entering into a previously unrecognized C-type inactivation state from which the recovery is slow.

Na^+ Permeation through Inactivated hERG Channels

We have recorded robust Na^+ current with Na^+-rich and K^+-free intracellular solution. The inactivation kinetics is very sensitive to permeating ions (Zhang et al., 2003a; Lin et al., 2005). K^+ free, Na^+ rich intracellular condition is very different from physiological solution. To establish our hypothesis that the hERG Na^+ current represents Na^+ permeating through the inactivated channels, it is fundamental to validate that hERG channels still display the characteristic fast, voltage-dependent inactivation under this extreme circumstance.

To address the hERG inactivation in the absence of K^+ but with 135 mM Na^+ in the pipette solution, the pulse protocols shown in Fig. 6 (A and B) were used. A bath solution contained 5 mM K^+ and 130 mM NMG^+ was used to study the hERG inactivation by monitoring the inward K^+ current. The hERG channels were inactivated by a holding potential of 60 mV. Repolarization to −100 mV (P1) induced channel recovery from the inactivated to the open state. Before deactivation, the cell membrane was depolarized to 20 mV (A) or 60 mV (B) with various durations (P2) to induce channel inactivation. The cell membrane voltage was then repolarized back to −100 mV (P3). The instantaneous inward current immediately after the membrane capacitive current upon P3 represents the fraction of not yet inactivated open channels, which decreases as the preceding depolarization to 20 or 60 mV (P2) prolonged (Fig. 6, A and B), reflecting the time-dependent inactivation occurring at depolarizing voltages (P2). Fitting the time course of the instantaneous current decrease gave a time constant for channel inactivation at 20 mV (Fig. 6 A) or 60 mV (Fig. 6 B). The time constants of inactivation at different depolarizing voltages were assessed and summarized in Fig. 6 D (●, n = 5). The voltage-dependent inactivation of hERG channels with 135 mM K^+ in the pipette solution (bath solution containing 5 mM K^+) was also evaluated using the standard triple pulse protocol (Fig. 6 C) and also plotted in Fig. 6 D (○, n = 4). Although the onset of hERG channel inactivation with 135 mM Na^+ in the pipette solution was faster than that with 135 mM K^+ in the pipette solution, hERG channels with 135 mM Na^+_i displayed unique fast, voltage-dependent inactivation similar to those with 135 mM K^+_i.

To directly address the hypothesis that the Na^+ permeation state is the initial P-type inactivated state, we performed experiments with a pipette solution containing 135 mM Na^+ (135 mM Na^+_i) and a bath solution containing 135 mM NMG^+ plus 1 mM K^+ (1 mM K^+_o). Under these recording conditions, depolarizing step to 80 mV evoked a small sustained outward Na^+ current

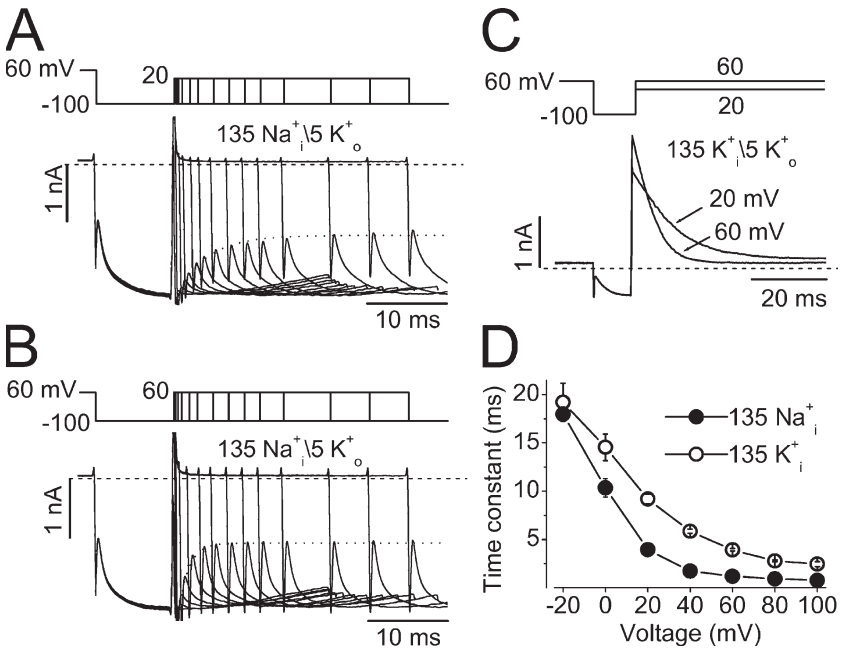

Figure 6. Voltage-dependent inactivation of hERG channels in the presence of 135 Na^+_i (A, B, and D) or 135 mM K^+_i (C and D). (A and B) hERG currents evoked by the voltage protocol shown above the traces to monitor the time-dependent channel inactivation at 20 (A) or 60 mV (B). hERG channels were inactivated at the holding potential of 60 mV. Repolarization to −100 mV (P1) caused channel recovery from inactivation. The membrane was depolarized to 20 or 60 mV with increasing durations (P2) to induce the voltage-dependent inactivation, which was judged by the instantaneous currents upon repolarization to −100 mV (P3) after P2. The instantaneous currents immediately after the cell capacitive current upon P3 were fitted to the single exponential function (dotted lines) to obtain the inactivation time constants. (C) Inactivation time courses of the hERG outward K^+ current at 20 or 60 mV. hERG channels were inactivated at the holding potential of 60 mV. Repolarization to −100 mV induced channel recovery from inactivation. The membrane was then depolarized to 20 or 60 mV to induce current inactivation, which was fitted to a single exponential function. (D) Inactivation time constant–voltage relationships of hERG channels under 135 Na^+_i/5 mM K^+_o (●, $n = 5$) or 135 mM K^+_i/5 mM K^+_o (○, $n = 4$).

(Fig. 7 A). The small amplitude of the outward Na^+ current resulted from the blocking effects of 1 mM K^+ in the external solution (see Fig. 2). Repolarizing steps elicited inward K^+ tail currents. Since K^+ only permeates through open channels, the shape of the inward tail current upon repolarization would provide us with critical information. If the Na^+ permeating state is the open state during the depolarizing step, the repolarization would evoke an instantaneous inward K^+ current. On the other hand, if the Na^+ permeating state is the fast P-type inactivated state, the tail current would display a rising phase, which reflects the fast P-type inactivated channels recovering to open state and then deactivating (recovery is faster than deactivation). The data shown in Fig. 7 (A–C) clearly indicate that the latter is the case. During depolarization to 80 mV, a sustained Na^+ current was recorded. Repolarizations to various voltages induced the inward tail currents, which displayed a rising phase before the current deactivation. The initial portion of the tail current is expanded in Fig. 7 B to show the rising phase of the tail currents. To obtain the recovery time constants, the rising phase of the tail current was fitted to a single exponential function. The time constants, which were plotted against the voltages in Fig. 7 C, displayed characteristic voltage dependence ($n = 6$). The voltage-dependent rising phase of the tail currents is usually referred to as the "hook," which is unique to hERG channels, and reflects the channel recovery from inactivated state to the open state. The recovery time constants of the hERG channel were also evaluated with a pipette solution containing 135 mM K^+ and a bath solution containing 135 mM NMG^+ plus 1 mM K^+ (135 mM K^+_i/1 mM K^+_o, Fig. 7, D–F, $n = 7$). Although recovery from inactivation of hERG channels is faster with 135 mM Na^+_i than that with 135 mM K^+_i, it is clear that the hERG channel displayed its unique fast voltage-dependent recovery from inactivation when the 135 mM Na^+-containing pipette solution was used.

In summary, data in Figs. 6 and 7 indicate that the hERG channel displayed its unique fast voltage-dependent inactivation and recovery from inactivation when a K^+-free, 135 mM Na^+ pipette solution was used. The onset of and recovery from inactivation described here is equivalent to the gating transitions between open and P-type inactivation state. The P-type inactivation state is likely the Na^+ permeating state.

If the Na^+ permeating state is the inactivated state, then accelerating inactivation would not significantly affect the Na^+ current because the inactivation is faster than activation in WT channels, and thus the channel activation is the rate-limiting step for the appearance of the Na^+ current upon depolarizations. On the other hand, disruption of fast (P-type) inactivation would eliminate the Na^+ permeation. These rationales were experimentally addressed below.

The T623A and S641A mutations have been reported to accelerate hERG channel inactivation (Mitcheson et al., 2000; Bian et al., 2004). We recently found that the F627Y mutation accelerates hERG inactivation (Guo et al., 2006). In T623A, F627Y, or S641A mutant channels, when a pipette solution containing 135 mM K^+

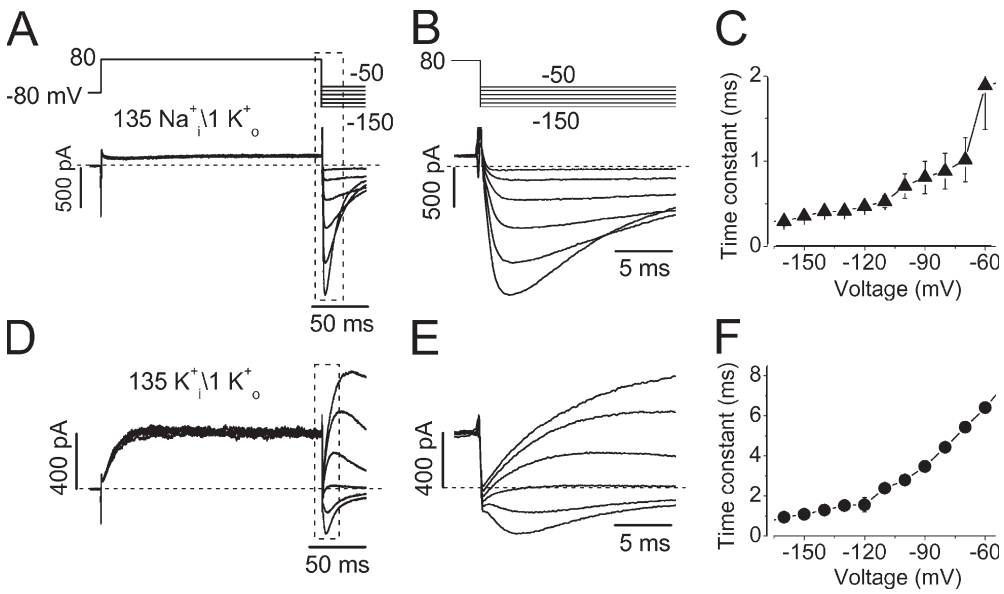

Figure 7. Recovery from inactivation of hERG channels under conditions of 135 mM Na^+_i/1 mM K^+_o (A–C) or 135 mM K^+_i/1 mM K^+_o (D–F). hERG currents were recorded with a bath solution containing 1 mM K^+ plus 135 mM NMG^+ and a pipette solution containing either 135 mM Na^+ (A–C) or 135 mM K^+ (D–F). (A) hERG outward Na^+ currents and the inward K^+ currents elicited by the voltage protocol above the current traces. (B) The expansion of initial phase of the tail currents in A. The rising phase of the tail current upon repolarization reflects the fast recovery of the inactivated channels to the open state before deactivation. The rising phase of the tail current was fitted to a single exponential function to obtain the time constant of recovery from inactivation (τ_{rec}) at each voltage. (C) The τ_{rec}–voltage relationships under 135 mM Na^+_i/1 mM K^+_o ($n = 6$). (D) hERG outward and inward K^+ currents elicited by the same voltage protocol shown at the top of A. (E) The expansion of initial phase of the tail currents in D. The rising phase of the tail current was fitted to a single exponential function to obtain the time constant of recovery from inactivation (τ_{rec}) at each voltage. (F) The τ_{rec}–voltage relationships under 135 mM K^+_i/1 mM K^+_o ($n = 7$).

was used, no K^+ current could be recorded with a bath solution containing 5 mM K^+_o, but WT channel current was robust (Fig. 8, left). As has been reported (Sanguinetti et al., 1995; Yang et al., 1997a), we found that removal of external K^+ led to a drastic reduction of the WT hERG channels (Fig. 8, right). (Please note the different scale bars for the top current traces. Also see the bottom panels for the summarized data.) Consistent with the C-type inactivation of the hERG Na^+ current (Fig. 4), two features of the WT K^+ current traces in the absence of K^+ suggest the entry into C-type inactivation of the channel when the "physiological" intracellular solution (135 mM K^+) was used. First, decays of the hERG current appear upon 4-s depolarizations (Fig. 8, right, top traces). Second, the tail current in the absence of K^+_o is much smaller than that in the presence of K^+_o. Because recovery from P-type inactivation is fast enough to generate unique hERG tail current, the small tail in the absence of K^+_o indicates that the majority of hERG channels had entered into a state from which recovery is not fast enough to generate tail current.

For T623A, F627Y, and S641A mutant hERG channels, as we confirmed below, the essentially absent K^+ current was due to the very fast entry into the P-type inactivated state. The absence of tail currents may also suggest that either the deactivation is accelerated or the recovery from inactivation is decelerated. To directly confirm that the absence of K^+ current in these mutant channels is a consequence of accelerated P-type inactivation, we investigated the gating kinetics of these channels. hERG K^+ currents were recorded under symmetrical 135 mM K^+ conditions under which inward tail currents were present upon repolarization to −80 mV after channel activation (Fig. 9, left). The decay of the tail currents was fitted to a single exponential function to estimate the deactivation time constant (τ_{deact}). It was found that τ_{deact} at −80 mV was 993.4 ± 264.9 ms for WT channels ($n = 5$), 62.3 ± 4.6 ms for T623A ($n = 7$), 151.4 ± 20.2 ms for F627Y ($n = 10$), and 94.7 ± 17.0 ms for S641A ($n = 8$). Thus, the deactivation was significantly accelerated in all three mutant channels ($P < 0.01$). We also analyzed the time course of recovery from inactivation in WT and mutant channels. The rising phase of the tail current at −80 mV was fitted to a single exponential function to obtain the time constant of recovery from inactivation (τ_{rec}). The τ_{rec} at −80 mV was 7.9 ± 0.8 ms ($n = 5$), 3.1 ± 0.3 ms ($n = 8$), 3.0 ± 0.3 ms ($n = 12$), and 2.9 ± 0.4 ms ($n = 8$) for WT, T623A, F627Y, and S641A channels, respectively. Thus, the recovery from inactivation was accelerated in the three mutant channels ($P < 0.01$). To construct the activation curve, the tail current peak amplitudes were plotted against the activation voltages and the data points were fitted to the Boltzmann equation. The voltage of half-activation of the channel ($V_{1/2}$) and the slope factor (k) were −11.6 ± 1.2 mV and 6.8 ± 0.4 mV for WT channels ($n = 5$), 2.9 ± 4.1 mV and 7.6 ± 0.6 mV for T623A ($n = 7$), −18.7 ± 3.9 mV and 8.7 ± 0.4 mV for F627Y ($n = 6$), and −4.2 ± 2.7 mV and 7.1 ± 0.4 mV for S641A ($n = 6$). Compared with WT channels, the $V_{1/2}$ of F627Y was not significantly changed ($P > 0.05$), and those of the T623A and S641A were slightly shifted in

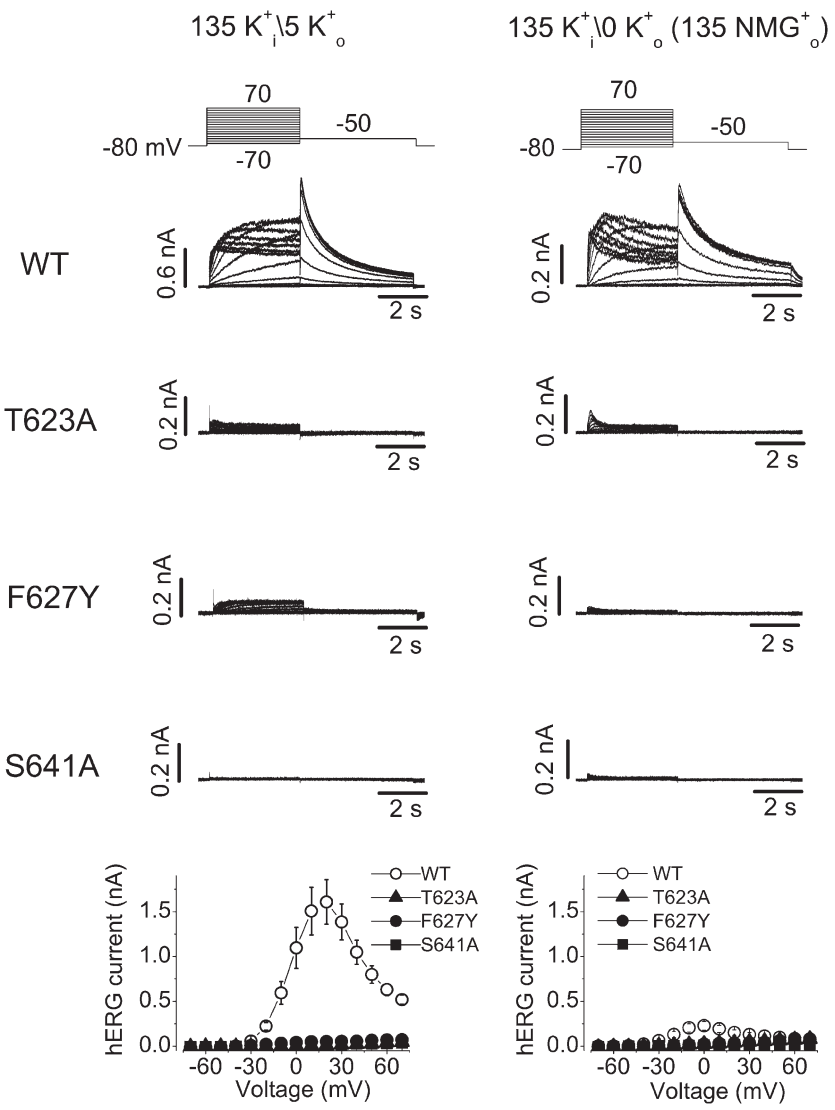

Figure 8. Families of WT, T623A, F627Y, and S641A hERG K^+ currents recorded in the presence of 5 mM K^+_o (left) or in the absence of K^+_o (NMG^+ as substitute, right). The pipette solution contained 135 mM K^+. In both panels, the voltage protocols are shown at the top and the current–voltage relationships are shown at the bottom. Changing external K^+ from 5 mM to 0 significantly reduced the WT hERG current (note the different bar scales in WT current traces in 0 and 5 mM K^+). In both 5 mM and 0 K^+_o conditions, no significant current could be recorded in the T623A, F627Y, and S641A mutant hERG channels (n = 4–7 cells).

the positive direction (Fig. 9, $P < 0.05$, bottom left). To evaluate inactivation time course of these mutant channels, a triple-pulse protocol was used. The hERG current decay during the test voltages was fitted to a single exponential function, and the time constant of inactivation (τ_{inact}) was plotted against the test voltages (Fig. 9, right). Compared with WT channels, inactivation was dramatically accelerated in all three mutants. For example, the τ_{inact} at 50 mV was increased by 12.6 (n = 7), 6.1 (n = 6), and 6.1-fold (n = 7) by the T623A, F627Y, and S641A mutation, respectively. These results indicate that the absence of hERG T623A, F627Y, and S641A K^+ currents at 0 or 5 mM K^+_o was due to an accelerated inactivation as well as an accelerated deactivation.

In contrast to K^+ currents, robust outward Na^+ currents were recorded in T623A, F627Y, and S641A channels (Fig. 10). The relative peak current–voltage relationships are shown in Fig. 10 B. The activation time courses of the Na^+ current in these three mutant channels were analyzed by single exponential fitting of the final rising portion of the current activation, a similar approach to that used in WT channels (Fig. 3). Whereas the activation time courses were similar between WT and S641A mutant Na^+ currents, activation time courses of T623A and F627Y were slower than that of WT channels (Fig. 10 C). Because the mutant T623A, F627Y, S641A channels displayed a significantly accelerated inactivation (Fig. 9), the presence of Na^+ current in these mutant channels strongly supports the notion that the Na^+ permeating state is the inactivated state.

To further address that the inactivation state is the Na^+ permeation state, we made the S631A mutation. This mutation is known to disrupt fast voltage-dependent hERG inactivation but retains high K^+ selectivity (Schönherr and Heinemann, 1996; Fan et al., 1999). We found that no detectable Na^+ current could be recorded in S631A inactivation-deficient channels (Fig. 11 A). The existence of S631A channels was confirmed by adding 1 mM

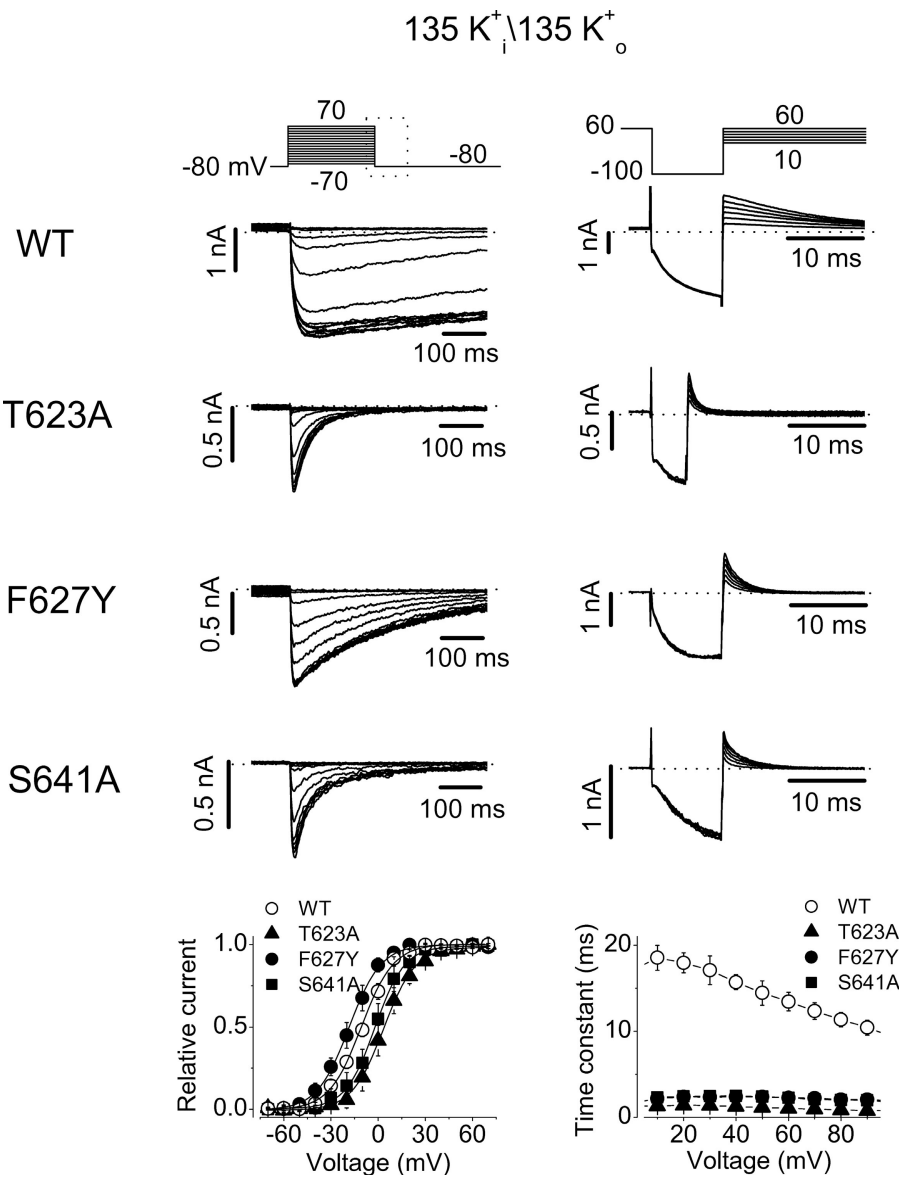

Figure 9. Gating properties of WT, T623A, F627Y, and S641A hERG channels in the symmetrical K^+ conditions. Both pipette and bath solutions contained 135 mM K^+. The voltage protocols are shown at the top of each panel. Left, activation properties of various hERG channels. Note that only a portion of the tail currents corresponding to the box area in the voltage protocol is shown. Peak tail currents were plotted against the test voltages and fitted to a Boltzmann function to obtain the activation curves. The rising and the decay phases of the tail currents were fitted to the single exponential function, respectively, to obtain the time constant of recovery from inactivation and to estimate the deactivation time course. Compared with WT channels, the deactivation of all three mutant channels was significantly faster. Right, inactivation properties of various hERG channels. The current decay upon each test voltage was fitted to a single exponential function to obtain the inactivation time constants (τ_{inact}), which are plotted against the depolarizing voltages at the bottom of the panel. The T623A, F627Y, and S641A mutations drastically accelerated hERG inactivation at all tested voltages.

K^+ to the bath solution, which caused an inward tail current upon repolarization to −80 mV without the rising phase that is present in WT channels (Fig. 11 B).

Inhibition of the hERG Na^+ Current by External Na^+ Ions

During the course of experiments, we were never able to record inward Na^+ current in WT hERG channels. We found that external Na^+ in fact potently blocks the hERG Na^+ current. As shown in Fig. 12 A, a family of Na^+ currents was recorded with a bath solution containing 135 mM NMG^+ (pipette solution contained 135 mM Na^+). When 10 mM Na^+ was added to the bath solution (NMG^+ was proportionally reduced), the Na^+ current was considerably reduced (Fig. 12 B). The reduction of the outward Na^+ current was not simply due to the decreased driving force because the maximal current was reduced and the inward Na^+ current never appeared. The concentration-dependent effects of external Na^+ on hERG Na^+ current were examined, and the half maximal concentration (IC_{50}) for external Na^+ to block the outward Na^+ current was 3.5 ± 0.4 mM (Fig. 12 C, $n = 8$). The Hill coefficient was 0.7, suggesting that one Na^+ ion binding to the channel can cause the block.

External Na^+ has been reported to block hERG K^+ current and the S624 residue was believed to be involved in the block (Mullins et al., 2002). We found that the S624A mutation removed the inhibitory effects of Na^+_o on the Na^+ current of hERG channels. In addition, we found that the F627Y and S641A mutations also abolished the blocking effects of external Na^+ on the hERG Na^+ current. However, Na^+_o still blocked the T623A Na^+ current with potency similar to WT channels (unpublished data). As can be seen in Fig. 13, in the symmetric Na^+ solutions (135 mM Na^+), no current

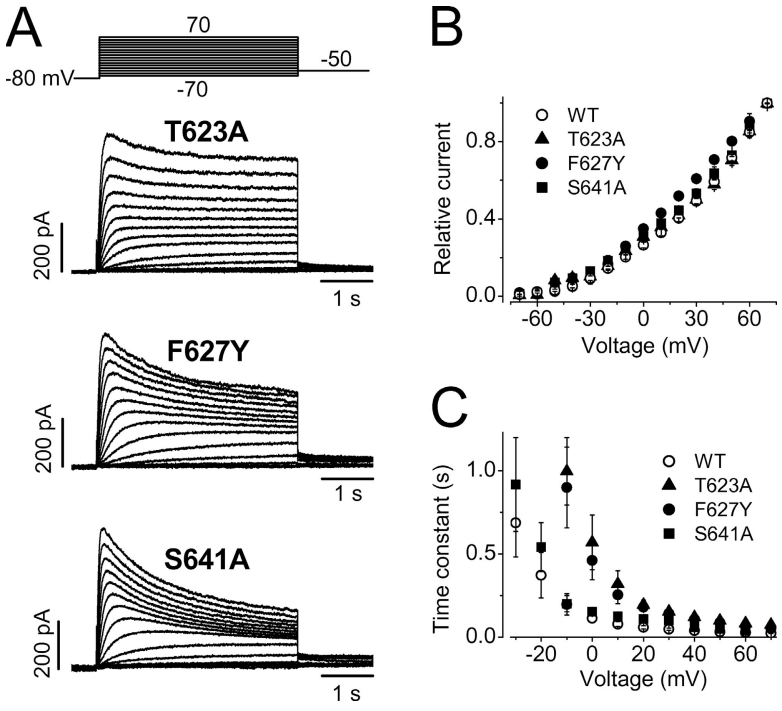

Figure 10. Na^+ currents recorded from the T623A, F627Y, and S641A mutant hERG channels. (A) Families of Na^+ currents from T623A, F627Y, and S641A. (B) The relative current–voltage relationships of Na^+ currents recorded from WT, T623A, F627Y, and S641A channels (n = 5–9 cells). (C) The activation time constant–voltage relationships of the T623A, F627Y, and S641A Na^+ currents (n = 5–9 cells), data for WT channels were also shown for comparison (n = 13).

could be detected in WT channels. In contrast, Na^+ currents were present in both inward and outward directions in mutant channels S624A, F627Y, and S641A (n = 4–9 cells for each mutation). Thus, although changes of the reversal potential at varying external Na^+ concentrations could not be determined in WT hERG channels due to the external Na^+ blocking effect, they were examined in S624A, F627Y, and S641A mutants (Fig. 14). The slope factor of the linear fit to the data was 39.8 ± 5.3 (n = 6) for S624A, 55.7 ± 3.7 (n = 4) for F627Y, and 46.9 ± 4.5 (n = 5) for S641A. Compared with the value (58.3) predicted by Nernst equation for Na^+ permeation, the slope factor for F627Y was not different and those for S624A and S641A were smaller ($P < 0.05$). Despite the difference, the fact that changing external Na^+ concentrations alters the reversal potentials of the Na^+ currents in these three mutant channels indicate that it is indeed Na^+ that permeates the mutant hERG channels.

To directly explore the state that Na^+_o permeates in the S624A, F627Y, and S641A mutant channels, we focused on the F627Y to investigate the inward Na^+ tail current and compared it with the K^+ tail current (Fig. 15). Following channel activation, the K^+ tail current displayed a rising phase, reflecting recovery of inactivated channels to the open state before deactivation (Fig. 15 B). In contrast, the Na^+ tail current did not display such a rising phase and reached the peak amplitude immediately upon repolarization and then deactivated (Fig. 15 A). These results indicate that Na^+ ions permeate through the inactivated state of F627Y channels. To examine the voltage dependence of the F627Y activation, the peak amplitudes of the tail currents were plotted against the depolarizing voltages, and g-V relationships were obtained (Fig. 15 C). It was

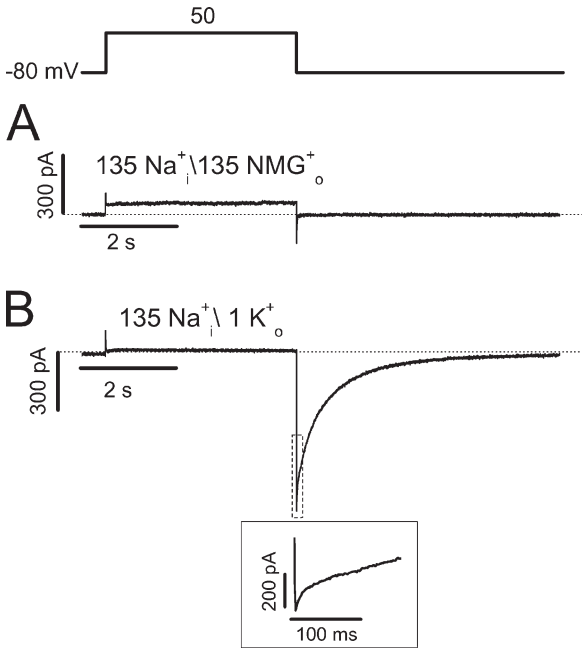

Figure 11. Absence of Na^+ current in the inactivation-deficient mutant hERG channel, S631A. (A) Current recorded with the pipette solution containing 135 mM Na^+ and the bath solution containing 135 mM NMG^+. (B) Current recorded with the similar condition but with 1 mM K^+ added to the bath solution (n = 4). The portion of the tail current in the dotted box is expanded in the inset to show the absence of the rising phase of the S631A K^+ tail current.

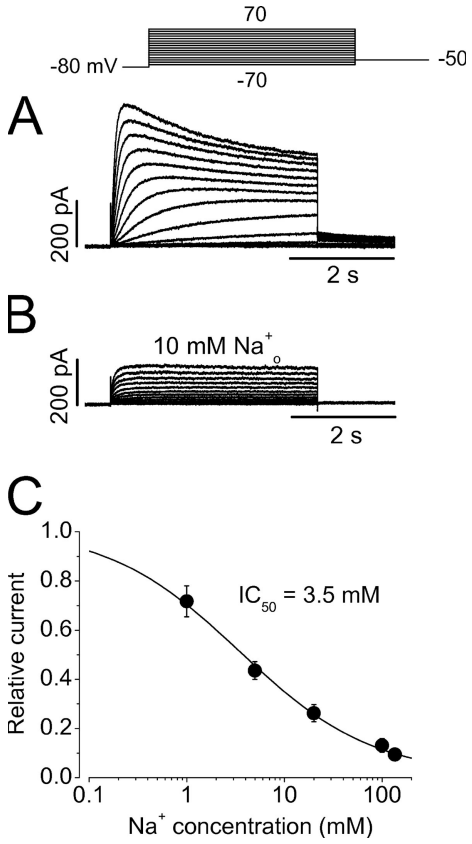

Figure 12. Inhibition of hERG Na^+ currents by external Na^+ ions (Na^+_o). (A and B) hERG Na^+ currents in the absence (A) and presence of 10 mM Na^+_o (B). The pipette solution contained 135 mM Na^+. (C) The concentration-dependent block of hERG Na^+ current by Na^+_o. The outward Na^+ currents at 50 mV at each Na^+_o relative to the control value were plotted against the Na^+_o concentration, and the data were fitted to the Hill equation ($n = 8$).

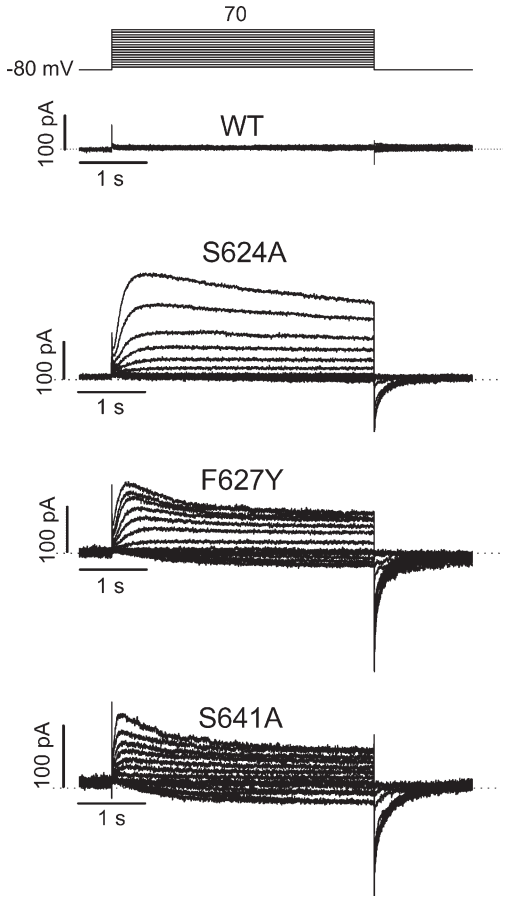

Figure 13. The S624A, F627Y, and S641A mutations eliminated Na^+_o-induced blockade of the hERG Na^+ current. Families of Na^+ currents from the WT, S624A, F627Y, and S641A channels in the symmetric Na^+ solutions (135 mM Na^+ in the pipette and bath solutions). The channels were activated by voltage steps from −70 to 70 mV in 10-mV increments from the holding potential of −80 mV. The cell was then clamped to −80 mV to elicit the tail currents. In contrast to WT channels, 135 mM Na^+_o did not block the S624A, F627Y, and S641A Na^+ currents that were present in both inward and outward directions.

found that the g-V relationship of the Na^+ current was bell shaped. The Na^+ tail current increased to reach the maximal value and then decreased following stronger depolarizations, indicating the entry into the stabilized C-type inactivation, from which recovery is slow. For K^+ current, the tail current reached the maximal value at 10 mV and remained constant at more positive voltages (Fig. 15 C). The g-V relations of the Na^+ and K^+ currents were fitted to the Boltzmann function. The $V_{1/2}$ and k of the K^+ current were -18.7 ± 0.9 mV and 8.8 ± 0.4 mV, respectively ($n = 6$), and the $V_{1/2}$ and k of the Na^+ current were -30.7 ± 1.6 mV and 6.7 ± 0.7 mV, respectively ($n = 6$). Thus, the $V_{1/2}$ of the Na^+ current is more negative than that of the K^+ current ($P < 0.01$).

DISCUSSION

The present study has demonstrated a robust Na^+ current in WT hERG channels. It is well known that hERG inactivation is voltage dependent; stronger depolarizations inactivate more channels. However, we found that stronger depolarization induced a larger outward Na^+ current in WT hERG channels. In the mutant T623A, F627Y, and S641A channels, the inactivation was accelerated to such an extent that outward K^+ current was not detectable under 0 or 5 mM K^+_o condition (Fig. 8). However, robust Na^+ currents were recorded in these mutant channels (Fig. 10). These results indicate that Na^+ permeates through an inactivated state of the hERG channel. Our data further showed that the hERG Na^+ current displayed an inactivation that is different from the well documented fast voltage-dependent hERG inactivation. This inactivation was slow (τ in a range of seconds) and displayed very weak voltage dependence. Recovery from this slow inactivation was also much slower than that of hERG K^+ current.

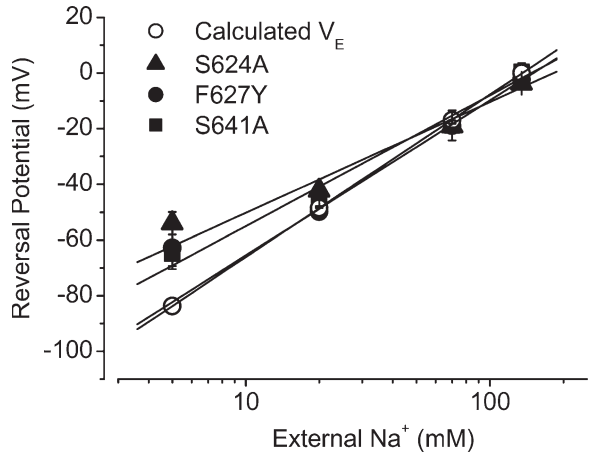

Figure 14. The reversal potentials of the S624A, F627Y, and S641A hERG channels under 135 mM intracellular Na^+ and varying external Na^+ concentrations. For each mutation, four to six cells were tested. The predicted reversal potential values were also shown.

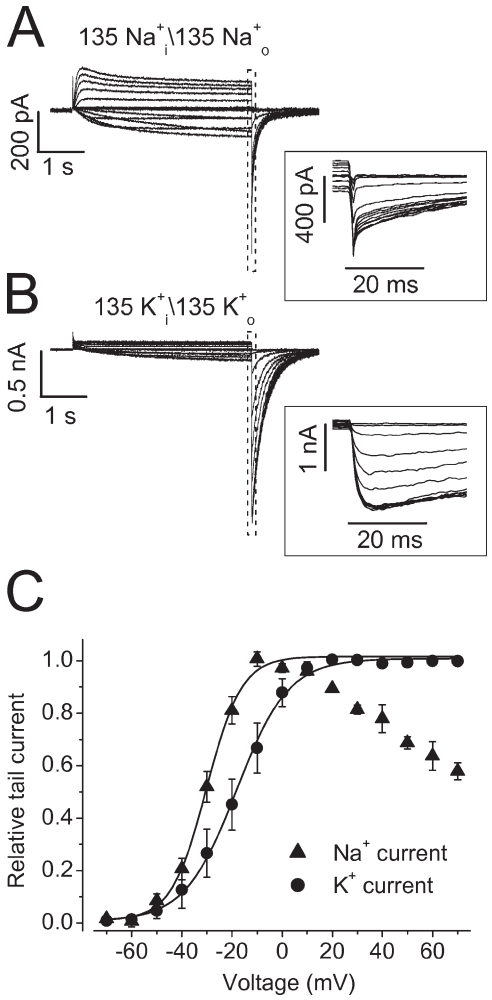

Figure 15. Comparison of the F627Y Na^+ and K^+ currents. Families of the Na^+ currents (Na^+_i/Na^+_o 135 mM, A) and K^+ currents (K^+_i/K^+_o 135 mM, B) from F627Y mutant channels. The channels were activated by voltage steps from −70 to 70 mV in 10-mV increments from the holding potential of −80 mV. The cell was then clamped to −80 mV to elicit the tail currents. The portions of the tail currents in the dotted box were expanded in the inset of A and B, respectively. The tail current–activation voltage relationships (g-V) were shown in C. The data points of K^+ currents at all tested voltages as well as those of Na^+ currents between −70 and −10 mV were fitted to the Boltzmann equation.

We propose that the hERG inactivation involves at least two steps, the P-type inactivation (I^P) and the C-type inactivation (I^C, Fig. 16). The well documented fast voltage-dependent inactivation of the hERG K^+ current may represent the I^P, but I^C has not been described possibly because it is prevented by external K^+ ions. As previously reported, K^+_o also slows the entry into I^P (Zhang et al., 2003a). We propose that I^P involves a constriction of the channel pore in a limited region, and this local conformational change excludes K^+ permeation. However, such partially constricted pore mouth allows passage of smaller Na^+ ions. I^P state is less stable and does not involve charge immobilization. The onset and recovery from I^P are fast. In our Na^+ current recording, I^P is manifested by the appearance of the Na^+ current. The slow inactivation of the Na^+ current represents transition from I^P to I^C, a stabilized state causing charge immobilization and involving a more substantial conformational change of the channel that locks the voltage sensor in an outward position. I^C is Na^+ impermeable. The onset and recovery from I^C are slow.

hERG gating scheme in Fig. 16 is supported by our experiments performed by using a pipette solution containing 135 mM Na^+ and a bath solution containing 1 mM K^+ (plus 135 mM NMG^+, Fig. 7). We have demonstrated that the hERG channel displayed its unique fast voltage-dependent inactivation and recovery from inactivation when a K^+ free, Na^+ rich intracellular solution was used (Figs. 6 and 7). During the depolarizing step in Fig. 7 A, an outward Na^+ current was observed. Upon repolarization, the inward K^+ currents were initially small and then increased in amplitude before deactivation. The rising phase of the hERG K^+ tail current reflects the fast inactivated (I^P) channels quickly recovering to open state and then deactivating (recovery from I^P is faster than deactivation). This result indicates that the Na^+ permeating state during depolarizing steps is the I^P. We have also demonstrated that the Na^+ current decays during prolonged depolarizing steps. This current decay may reflect the slow entry into the more stable inactivated state I^C from which recovery is slow (Figs. 4 and 5). The insight for the Na^+ permeation state was also obtained from the F627Y mutant channel. Since the F627Y mutation removed the external Na^+ blocking effect, the inward Na^+ tail current could be recorded (Figs. 13 and 15). The F627Y Na^+ tail current upon repolarization did not display a rising phase (Fig. 15 A). Yet, during repolarization, the I^P-inactivated

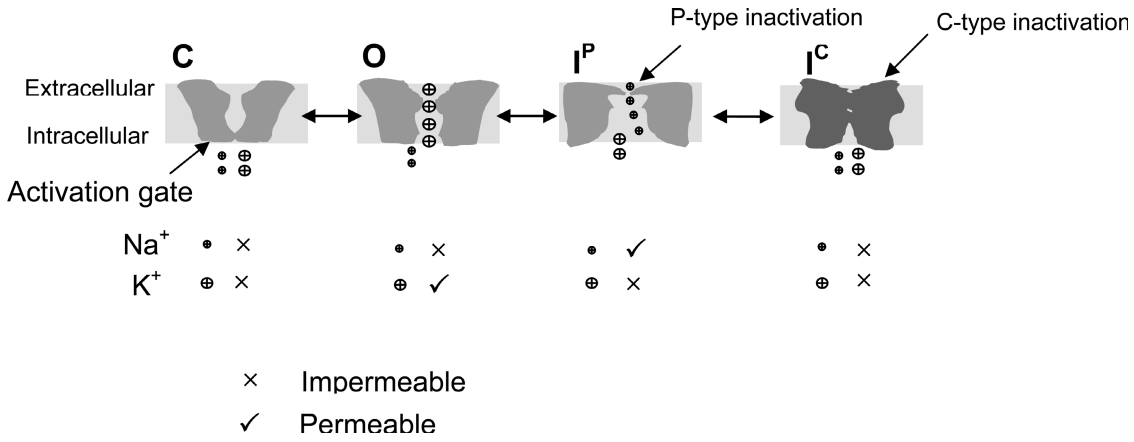

Figure 16. Proposed hERG gating scheme. I^P is the only state that conducts Na^+.

F627Y channels recover to open before deactivation as evidenced by the rising phase of the inward K^+ tail current (Fig. 15 B). Thus, the absence of the rising phase of the Na^+ current indicates that the Na^+ permeating state is not the open state. The absence of Na^+ permeation through open hERG channels is also supported by the experiments shown in Fig. 4 (C and D). After a large outward Na^+ current was induced by a depolarization to 70 mV, changing depolarizing voltage to less positive voltages induces a quick decay of the Na^+ currents, reflecting some channels exiting the inactivated state and traveling into the open state. Consistently, the time constants of this fast decay are in millisecond ranges similar to the time constants of recovery from inactivation shown in Fig. 7. As well, in S631A inactivation-deficient channels, depolarization failed to evoke any Na^+ current. However, the S631A channels were apparently in the open state during the depolarizing pulse since adding 1 mM K^+ to the bath solution caused a large inward tail current that occurred immediately upon repolarization without a rising phase (Fig. 11). These results suggest that Na^+ does not significantly permeate through open channels.

We conclude that Na^+ permeates through the I^P-inactivated channels but not through the closed (resting), open, or I^C-inactivated channels. We have found that the channel inactivation rate has been accelerated by 6.1–12.6-fold in T623A, F627Y, and S641A mutations (Fig. 9). We also found that the activation time course of the S641A Na^+ current was not different from that of WT currents, and the activation time courses of the T623A and F627Y Na^+ currents were slower than that of WT Na^+ currents (Fig. 10 C). The slowed activation rate in T623A and F627Y mutants that displayed accelerated inactivation indicates that hERG channel does not directly enter into the inactivated state from the closed state. Instead, hERG channel must go through the open state to enter into inactivation states. Consistently, because onset of hERG P-type inactivation is much faster than channel activation (Figs. 3, 7, 9, and 10), the rate-limiting step of activation rates of the Na^+ currents is likely determined by the closed to open transition.

The concept that the I^P-inactivated state is the Na^+ permeating state is consistent with the data from *Shaker* channels. It was reported that the permeability of Na^+ ions through the open K^+ channel is negligible. However, the permeation properties change during inactivation and favor Na^+ permeation (Starkus et al., 1997a; Wang et al., 2000; Zhang et al., 2003b). It has been shown that the high Na^+ permeability state is an intermediate state between the open and deep C-type inactivated states in Kv1.5 channels (Wang et al., 2000).

There are some differences between *Shaker* and hERG K^+ current inactivation. The onset of *Shaker* C-type inactivation is slower than that of hERG and is not obviously voltage dependent (Rasmusson et al., 1998). In contrast, onset of inactivation of hERG is very fast and strongly voltage dependent (Smith et al., 1996; Spector et al., 1996). The difference between hERG and *Shaker* inactivation may be due to the fact that hERG has a more flexible pore. There are 43 amino acids in hERG S5-P linker whereas there are 14–18 amino acids in the corresponding region of most other Kv channels (Dun et al., 1999). In addition, the *Shaker* sequence has double tryptophans (WW) at the NH_2-terminal end of the pore loop, and a tyrosine (Y) in the "signature motif" (GYG) at the COOH-terminal end. According to the crystal structure of KcsA, a model K^+ channel, hydrogen bonds can be formed in the three-dimensional structure around the outer mouth between the nitrogens of "WW" and the hydroxyl group of "Y" of the four subunits. These hydrogen bonds serve as molecular springs, which pull the pore wall radially outward to hold the outer mouth open at its proper diameter (Doyle et al., 1998). Such hydrogen bonds seem so important that a single mutation of tryptophan to phenylalanine in *Shaker* (ShH4-IR W434F) or Kv1.5 (W472F) makes these channels nonconductive to K^+ due to the

extremely fast entry into an inactivated state perhaps equivalent to I^P (Perozo et al., 1993; Chen et al., 1997; Yang et al., 1997b). Whereas no K^+ current would be detected, Na^+ current was present in the W434F Shaker and W472F Kv1.5 channels (Starkus et al., 1998; Wang and Fedida, 2002). As mentioned, the W434F *Shaker* and W472F Kv1.5 are not in a charge-immobilized I^C equivalent state. The corresponding tryptophans and tyrosine are missing in hERG. The absence of hydrogen bonds and long S5-P linker may lead to a more flexible pore (Tseng, 2001). Consequently, hERG channels are more prone to enter into the less stable P-type inactivated state I^P. Recently, Berneche and Roux (2005) presented a model that couples the rate of inactivation with ion occupancy in the selectivity filter. According to the model, there is a modest rearrangement that leads to a nonconducting conformational state of the selectivity filter, which is then effectively acting as a gate. This structural rearrangement involves only one of the four subunits at a time, breaking the fourfold symmetry of the channel. The first step, which initiates the conformational transition toward the nonconducting state, is very sensitive to the configurations of the ion occupying the selectivity filter. Membrane depolarization (positive voltage shift) favors a state in which the transition can take place, and membrane polarization (negative voltage shift) favors a state that prevents the transition. This model could potentially explain the voltage dependence of hERG inactivation (Berneche and Roux, 2005). However, the voltage dependence of inactivation is not generally obvious in *Shaker*-related K^+ channels (Rasmusson et al., 1998). The lack of strong voltage dependence of the typical C-type inactivation of *Shaker* channels may be due to the hydrogen bonds between the tyrosine from the GYG moiety and a tryptophan from an adjacent subunit, corresponding to Tyr78 and Trp68 in KcsA, which offset the voltage dependence of the structural rearrangement leading to the nonconducting conformation state.

While the I^P inactivation may correspond to the fast inactivation in K^+ current recordings, I^C inactivation of hERG has not been described in the K^+ current recordings. It is known that external K^+ inhibits P/C-type inactivation (Zhang et al., 2003a,b, 2005). It has been reported (Sanguinetti et al., 1995; Yang et al., 1997a) and we have confirmed (Fig. 8) that reduction of K^+_o significantly decreases hERG current amplitude. Although lowering K^+_o accelerates the fast inactivation of hERG channels (Wang et al., 1996, 1997; Zhang et al., 2003a), and this effect was initially thought to be responsible for the effect of K^+_o on the hERG current magnitude (Yang et al., 1997a), a quantitative analysis by Wang et al. (1997) suggested that the changed fast-inactivation rate is not responsible for the altered current amplitude. Presently, the mechanism of K^+_o-dependent changes of the HERG current amplitude is not known, and we believe that the entry into the slow C-type inactivation at low K^+_o is responsible for this phenomenon as supported by our data shown in Fig. 8.

The reason why fast inactivated hERG channels are not permeable to K^+ but permeable to Na^+ is not known. It seems that the conformational change of the serine side chain at 631 during inactivation is involved. Previously, Ulens et al. (1999) have reported that 250 μM norpropoxyphene, the major metabolite of propoxyphene, increased Na^+ permeability by 30-fold in WT hERG channels but not in S631C mutant channels, suggesting that norpropoxyphene may interact with S631 to increase the hERG Na^+ permeability. Fan et al. (1999) reported that S631K and S631E mutations significantly increased the hERG Na^+ permeability. Therefore, we believe that the inactivation-associated conformational change of the Ser-631 may contribute to the increased Na^+ permeability during the inactivation process. This notion is also consistent with our data that there is no Na^+ current in the S631A mutant channel (Fig. 11).

In WT hERG channels, while robust outward Na^+ current was recorded with a pipette solution containing 135 mM Na^+ and a bath solution containing 135 mM NMG^+ (Figs. 1–5), no Na^+ current could be detected when a 135 mM Na^+-containing bath solution was used. We found that external Na^+ potently blocks the Na^+ current in a concentration-dependent manner (IC_{50} = 3.5 mM, Fig. 12). The Na^+_o block of hERG K^+ currents has been reported previously (Mullins et al., 2002), and the IC_{50} value for Na^+_o to block the hERG Na^+ current is close to that for Na^+_o to block hERG K^+ currents (Mullins et al., 2002). It was also reported that the S624A and S624T mutations removed the Na^+_o blocking effect on the hERG K^+ current (Mullins et al., 2002). It was proposed that Na^+_o-induced block resulted from the competition between extracellular sodium and potassium for the hERG channel pore, and that mutations of S624A and S624T increased the K^+ occupancy of the most outer pore site, which resulted in both impaired inactivation and decreased sensitivity to inhibition by Na^+_o in the two mutant channels (Mullins et al., 2002). In the present study, we found that the S624A mutation also removed Na^+_o block of the hERG Na^+ current. We further found that the F627Y and S641A removed Na^+_o blocking effects on the hERG Na^+ current as well. Since the F627Y and S641A significantly accelerated hERG inactivation, whereas S624A slightly decelerated it (unpublished data; also see Mullins et al., 2002), inactivation gating seems not to be involved in the Na^+_o block of hERG channels. Also, since our experiments were performed in the absence of K^+, it ruled out competition between Na^+_o and K^+_o for the binding to the hERG channel pore as a mechanism for Na^+_o-induced hERG block. In the paper published by Mullins et al. (2002), it was also mentioned that Na^+ current through hERG channels could not be detected (Mullins et al., 2002).

The reason for the discrepancy is not known but may be related to the Na^+_o blocking effect. The exact mechanism of Na^+_o block of hERG Na^+ current is not known. It seems that the binding domain is located in the outer mouth of the channel pore since only external Na^+ can produce blocking effects. Mutations at the S624, F627 or S641 position of hERG may induce a conformational change that disrupts the binding domain for Na^+_o to cause block.

Although Na^+_o blocked hERG Na^+ current, a robust outward hERG Na^+ current indicates that intracellular Na^+ (Na^+_i) does not block the channels. This is in contrast to the effects of Na^+ ions on other voltage-gated K^+ channels. Na^+_i is known to block several voltage-gated K^+ channels, including rat ether-a-go-go (rEAG K^+ channel) (Yellen, 1984; Pardo et al., 1998; Pusch et al., 2001). On the other hand, Na^+_o generally does not block voltage-gated K^+ channels (Hille, 2001). Similarly, Na^+_i, but not Na^+_o, blocks the bacterial channel KcsA in lipid bilayers and the K^+-selective prokaryotic glutamate receptor GluR0. Sidedness of Na^+ block in these channels has been used to determine the channel topology (Chen et al., 1999; Heginbotham et al., 1999). Clearly, Na^+ block of hERG channels displayed a sidedness opposite to most K^+ channels. The mechanisms of Na^+ block of hERG channels need further investigation.

In conclusion, by studying the Na^+ currents in hERG channels, we propose that there are at least two distinct inactivated states in hERG channels, the initial P-type and the more stable C-type inactivated state. The Na^+ permeation and block of hERG channels provide a novel way to extend our understanding of hERG channel gating and modulation.

We thank Dr. Craig T. January (University of Wisconsin) for the stable hERG cell line and Dr. Gail A. Robertson for the hERG cDNA.

This project was supported by a grant (MOP-72911) from the Canadian Institutes of Health Research to Shetuan Zhang who is a recipient of the New Investigator Award from the Heart and Stroke Foundation of Canada. Hongying Gang is a Master of Science graduate student.

Olaf S. Andersen served as editor.

Submitted: 30 January 2006
Accepted: 1 June 2006

REFERENCES

Almers, W., and C.M. Armstrong. 1980. Survival of K^+ permeability and gating currents in squid axons perfused with K^+-free media. *J. Gen. Physiol.* 75:61–78.

Berneche, S., and B. Roux. 2005. A gate in the selectivity filter of potassium channels. *Structure.* 13:591–600.

Bian, J.S., J. Cui, Y. Melman, and T.V. McDonald. 2004. S641 contributes HERG K^+ channel inactivation. *Cell Biochem. Biophys.* 41:25–40.

Bianchi, L., B. Wible, A. Arcangeli, M. Taglialatela, F. Morra, P. Castaldo, O. Crociani, B. Rosati, L. Faravelli, M. Olivotto, and E. Wanke. 1998. HERG encodes a K^+ current highly conserved in tumors of different histogenesis-a selective advantage for cancer cells. *Cancer Res.* 58:815–822.

Chen, F.S.P., D. Steele, and D. Fedida. 1997. Allosteric effects of permeating cations on gating currents during K^+ channel deactivation. *J. Gen. Physiol.* 110:87–100.

Chen, G.Q., C. Cui, M.L. Mayer, and E. Gouaux. 1999. Functional characterization of a potassium-selective prokaryotic glutamate receptor. *Nature.* 402:817–821.

De Biasi, M., H.A. Hartmann, J.A. Drewe, M. Taglialatela, A.M. Brown, and G.E. Kirsch. 1993. Inactivation determined by a single site in K^+ pores. *Pflugers Arch.* 422:354–363.

Doyle, D.A., J.M. Cabral, R.A. Pfuetzner, A.L. Kuo, J.M. Gulbis, S.L. Cohen, B.T. Chait, and R. MacKinnon. 1998. The structure of the potassium channel: molecular basis of K^+ conduction and selectivity. *Science.* 280:69–77.

Dun, W., M. Jiang, and G.N. Tseng. 1999. Allosteric effects of mutations in the extracellular S5-P loop on the grating and ion permeation properties of the hERG potassium channel. *Pflugers Arch.* 439:141–149.

Fan, J.S., M. Jiang, W. Dun, T.V. McDonald, and G.N. Tseng. 1999. Effects of outer mouth mutations on *hERG* channel function: a comparison with similar mutations in the *Shaker* channel. *Biophys. J.* 76:3128–3140.

Faravelli, L., A. Arcangeli, M. Olivotto, and E. Wanke. 1996. A HERG-like K^+ channel in rat F-11 DRG cell line: pharmacological identification and biophysical characterization. *J. Physiol.* 496:13–23.

Guo, J., H. Gang, and S. Zhang. 2006. Molecular determinants of cocaine block of hERG potassium channels. *J. Pharmacol. Exp. Ther.* 317:865–874.

Heginbotham, L., M. LeMasurier, L. Kolmakova-Partensky, and C. Miller. 1999. Single *Streptomyces lividans* K^+ channels: functional asymmetries and sidedness of proton activation. *J. Gen. Physiol.* 114:551–559.

Herzberg, I.M., M.C. Trudeau, and G.A. Robertson. 1998. Transfer of rapid inactivation and sensitivity to the class III antiarrhythmic drug E-4031 from HERG to M-eag channels. *J. Physiol.* 511:3–14.

Hille, B. 2001. Ionic Channels of Excitable Membranes. Third edition. Sinauer Associates Inc., Sunderland, MA. 814 pp.

Ho, S.N., H.D. Hunt, R.M. Horton, J.K. Pullen, and L.R. Pease. 1989. Site-directed mutagenesis by overlap extension using the polymerase chain reaction. *Gene.* 77:51–59.

Hoshi, T., W.N. Zagotta, and R.W. Aldrich. 1991. Two types of inactivation in *Shaker* K^+ channels: effects of alterations in the carboxy-terminal region. *Neuron.* 7:547–556.

Keating, M.T., and M.C. Sanguinetti. 2001. Molecular and cellular mechanisms of cardiac arrhythmias. *Cell.* 104:569–580.

Kiss, L., J. LoTurco, and S.J. Korn. 1999. Contribution of the selectivity filter to inactivation in potassium channels. *Biophys. J.* 76:253–263.

Korn, S.J., and S.R. Ikeda. 1995. Permeation selectivity by competition in a delayed rectifier potassium channel. *Science.* 269:410–412.

Lin, J., J. Guo, H. Gang, P. Wojciechowski, J.T. Wigle, and S. Zhang. 2005. Intracellular K^+ is required for the inactivation-induced high affinity binding of cisapride to HERG channels. *Mol. Pharmacol.* 68:855–865.

Loots, E., and E.Y. Isacoff. 1998. Protein rearrangements underlying slow inactivation of the *Shaker* K^+ channel. *J. Gen. Physiol.* 112:377–389.

Melishchuk, A., A. Loboda, and C.M. Armstrong. 1998. Loss of *Shaker* K channel conductance in 0 K^+ solutions: role of the voltage sensor. *Biophys. J.* 75:1828–1835.

Mitcheson, J.S., J. Chen, M. Lin, C. Culberson, and M.C. Sanguinetti. 2000. A structural basis for drug-induced long QT syndrome. *Proc. Natl. Acad. Sci. USA.* 97:12329–12333.

Mullins, F.M., S.Z. Stepanovic, R.R. Desai, A.L. George Jr., and J.R. Balser. 2002. Extracellular sodium interacts with the HERG channel at an outer pore site. *J. Gen. Physiol.* 120:517–537.

Olcese, R., R. Latorre, L. Toro, F. Bezanilla, and E. Stefani. 1997. Correlation between charge movement and ionic current during slow inactivation in *Shaker* K^+ channels. *J. Gen. Physiol.* 110:579–589.

Pardo, L.A., A. Bruggeman, J. Camacho, and W. Stühmer. 1998. Cell cycle–related changes in the conducting properties of r-eag K^+ channels. *J. Cell Biol.* 143:767–775.

Perozo, E., R. MacKinnon, F. Bezanilla, and E. Stefani. 1993. Gating currents from a non-conducting mutant reveal open-closed conformation in Shaker K^+ channels. *Neuron.* 11:353–358.

Pusch, M., L. Ferrera, and T. Friedrich. 2001. Two open states and rate-limiting gating steps revealed by intracellular Na+ block of human KCNQ1 and KCNQ1/KCNE1 K+ channels. *J. Physiol.* 533:135–143.

Rasmusson, R.L., M.J. Morales, S. Wang, S. Liu, D.L. Campbell, M.V. Brahmajothi, and H.C. Strauss. 1998. Inactivation of voltage-gated cardiac K^+ channels. *Circ. Res.* 82:739–750.

Sanguinetti, M.C., C. Jiang, M.E. Curran, and M.T. Keating. 1995. A mechanistic link between an inherited and an acquired cardiac arrhythmia: *HERG* encodes the I_{Kr} potassium channel. *Cell.* 81:299–307.

Sanguinetti, M.C., and N.K. Jurkiewicz. 1990. Two components of delayed rectifier K^+ current: differential sensitivity to black by class III antiarrhythmic agents. *J. Gen. Physiol.* 96:195–215.

Schönherr, R., and S.H. Heinemann. 1996. Molecular determinants for activation and inactivation of HERG, a human inward rectifier potassium channel. *J. Physiol.* 493:635–642.

Smith, P.L., T. Baukrowitz, and G. Yellen. 1996. The inward rectification mechanism of the HERG cardiac potassium channel. *Nature.* 379:833–836.

Spector, P.S., M.E. Curran, A.R. Zou, and M.C. Sanguinetti. 1996. Fast inactivation causes rectification of the I_{Kr} channel. *J. Gen. Physiol.* 107:611–619.

Starkus, J.G., L. Kuschel, M.D. Rayner, and S.H. Heinemann. 1997. Ion conduction through C-type inactivated *Shaker* channels. *J. Gen. Physiol.* 110:539–550.

Starkus, J.G., L. Kuschel, M.D. Rayner, and S.H. Heinemann. 1998. Macroscopic Na^+ currents in the "nonconducting" *Shaker* potassium channel mutant W434F. *J. Gen. Physiol.* 112:85–93.

Trudeau, M.C., J.W. Warmke, B. Ganetzky, and G.A. Robertson. 1995. HERG, a human inward rectifier in the voltage-gated potassium channel family. *Science.* 269:92–95.

Tseng, G.N. 2001. I_{Kr}: the hERG channel. *J. Mol. Cell. Cardiol.* 33:835–849.

Ulens, C., P. Daenens, and J. Tytgat. 1999. Norpropoxyphene-induced cardiotoxicity is associated with changes in ion-selectivity and gating of HERG currents. *Cardiovasc. Res.* 44:568–578.

Wang, S., M.J. Morales, S. Liu, H.C. Strauss, and R.L. Rasmusson. 1996. Time, voltage and ionic concentration dependence of rectification of h-erg expressed in *Xenopus* oocytes. *FEBS Lett.* 389:167–173.

Wang, S.M., S.G. Liu, M.J. Morales, H.C. Strauss, and R.L. Rasmusson. 1997. A quantitative analysis of the activation and inactivation kinetics of *HERG* expressed in *Xenopus* oocytes. *J. Physiol.* 502:45–60.

Wang, Z., and D. Fedida. 2001. Gating charge immobilization caused by the transition between inactivated states in the Kv1.5 channel. *Biophys. J.* 81:2614–2627.

Wang, Z., and D. Fedida. 2002. Uncoupling of gating charge movement and closure of the ion pore during recovery from inactivation in the Kv1.5 channel. *J. Gen. Physiol.* 120:249–260.

Wang, Z.R., J.C. Hesketh, and D. Fedida. 2000. A high-Na^+ conduction state during recovery from inactivation in the K^+ channel Kv1.5. *Biophys. J.* 79:2416–2433.

Yang, T., D.J. Snyders, and D.M. Roden. 1997a. Rapid inactivation determines the rectification and $[K^+]_o$ dependence of the rapid component of the delayed rectifier K^+ current in cardiac cells. *Circ. Res.* 80:782–789.

Yang, Y.S., Y.Y. Yan, and F.J. Sigworth. 1997b. How does the W434F mutation block current in *Shaker* potassium channels. *J. Gen. Physiol.* 109:779–789.

Yellen, G. 1984. Relief of Na^+ block of Ca^{2+}-activated K^+ channels by external cations. *J. Gen. Physiol.* 84:187–199.

Zhang, S., C. Eduljee, D.C. Kwan, S.J. Kehl, and D. Fedida. 2005. Constitutive inactivation of the hKv1.5 mutant channel, H463G, in K^+-free solutions at physiological pH. *Cell Biochem. Biophys.* 43:221–230.

Zhang, S., S.J. Kehl, and D. Fedida. 2003a. Modulation of human ether-a-go-go-related K^+ (HERG) channel inactivation by Cs^+ and K^+. *J. Physiol.* 548:691–702.

Zhang, S., H.T. Kurata, S.J. Kehl, and D. Fedida. 2003b. Rapid induction of P/C-type inactivation is the mechanism for acid-induced K^+ current inhibition. *J. Gen. Physiol.* 121:215–225.

Zhou, Z., Q. Gong, B. Ye, Z. Fan, J.C. Makielski, G.A. Robertson, and C.T. January. 1998. Properties of HERG channels stably expressed in HEK 293 cells studied at physiological temperature. *Biophys. J.* 74:230–241.